UNIVERSITY HONORS PROGRAM
SENIOR PROJECT- APPROVAL

Name: Jamie N. Jones

College: Arts and Sciences Department: Chemistry

Faculty Mentor: Dr. Craig E. Barnes

Project Title: Use of X-ray Diffraction in the Determination of the Crystal Structure of $(Co(C_5H_5))_3(CO)_2$ and $[Zr_6I_{12}B(CH_3OH)_6][I(CH_3OH)_6]$

I have reviewed this completed senior honors thesis with this student and certify that it is a project commensurate with honors level undergraduate research in this field.

Signed: Craig E Barnes, Faculty Mentor

Date: May 9, 2000

Comments (Optional):

Use of X-ray Diffraction in the Determination of the Crystal Structure of $(Co(C_5H_5))_3(CO)_2$ and $[Zr_6I_{12}(CH_3OH)_6][I(CH_3OH)_6]$

A Senior Thesis Prepared for the

Honors Bachelor of Science in Chemistry Degree

University of Tennessee, Knoxville

Jamie N. Jones

May 2000

ACKNOWLEDGMENTS

The author would like to thank Dr. Craig E. Barnes for his support of her research. Each member of the Barnes' group has significantly contributed to the author's education. The time and patience they devoted to answering questions and teaching methods and techniques enhanced the author's undergraduate research experience and is greatly appreciated. Special thanks go to John Clavier and Suree Saengkerdsub for their NMR instruction.

The author's parents and sister have given unconditional support, encouragement, and love. (Thanks, Mom, for the marshmallows and toothpicks to make my cluster "models".) Without a loving family the author's undergraduate education would not have been possible.

Aristotle once said, "Without friends no one would choose to live, though he had all other goods." The author has been blessed with wonderful friends who have made the journey a pleasant one. Many thanks go to Monica Collins, Sarah Brown, Joel Hatchett, and Eric Bliss.

ABSTRACT

X-ray diffraction is an important technique for determining the structure of a compound. In two separate studies, X-ray diffraction will be used to understand the structure of inorganic complexes in the crystalline state. The two discussed topics include a study of the temperature dependence of the structure of $(CoCp)_3(CO)_2$ and the structure determination of a novel, single crystal zirconium halide solid-state cluster.

Unsaturated trinuclear metal complexes from group 9 metals, cobalt, rhodium, and iridium, are unusual and exhibit interesting properties because they are composed of electron-rich metals in an electron deficient environment. The extremely reactive, 46 electron, $(CpCo)_3(CO)_2$ cluster is especially unique since previous magnetic susceptibility studies have indicated that the crystalline solid undergoes a magnetic phase change in the temperature range of -100 to -150°C. At temperatures above -100°C $(CpCo)_3(CO)_2$ is paramagnetic. Between -100 and -150°C the paramagnetic susceptibility of the cluster drops until it becomes fully diamagnetic below -150°C. In an attempt to correlate structure with magnetic behavior, a single crystal X-ray diffraction study was conducted to examine how the unit cell constants and the molecular structure changed with temperature. We observed that the a-b axes of the unit cell experienced a greater contraction in the -90 to -120°C range than did the c axis. This change in the unit cell and Co—Co bond distance in the complex correlates well with the magnetic behavior of this complex in the solid state. A description of the structure and magnetic properties of $(CpCo)_3(CO)_2$ will be presented.

Exploration of the solution chemistry of $Zr_6I_{14}B$ yielded a procedure for producing more soluble polycrystalline cluster material. Due to the high cross-linkage of the iodide ligands the

$Zr_6I_{14}B$ cluster was found to dissolve slowly in deoxygenated water. Addition of hydrochloric acid yielded a polycrystalline material, which was more readily soluble in methanol. From the methanol solution single crystals were produced. X-ray diffraction of the single crystals determined the chemical formula of the compound to be $[Zr_6I_{12}B(CH_3OH)_6][I(CH_3OH)_6]$. The crystal was hexagonal and in the $R\bar{3}$ space group. The unit cell lengths were determined to be a = 17.710(2)Å and c = 13.915(2)Å. There are three cluster molecules per unit cell, Z=3. A comparative look at the boron-centered halide family of hexazirconium clusters indicated a decrease in the Zr—X bond length as the halide size increased. The increased size of the halogen atom forces an extention of the zirconium cage causing the X—Zr—X bond angle to become more acute.

TABLE OF CONTENTS

LIST OF TABLES

LIST OF FIGURES

CHAPTER I

Introduction

Two independent topics will be addressed in this thesis. The first being the synthesis and temperature dependent study of the structural properties of crystalline $(Co(C_5H_5))_3(CO)_2$ and the second the synthesis and excision of the solid-state cluster $KZr_6I_{14}B$. Each involves the use of standard organometallic synthetic methods and utilization of X-ray diffraction as a characterization tool.

Figure 1.1 depicts the trinuclear cobalt compound $(Co(C_5H_5))_3(CO)_2$, which for brevity will be abbreviated as trinuclear **1** throughout this work. $(Co(C_5H_5))_3(CO)_2$ is one member of a series of carbonyl-capped, trinuclear metal clusters. These clusters have been the object of extensive study since the discovery of the trinickel complex $Ni(C_5H_5))_3(CO)_2$ by Fischer and Palm.[1] The series of clusters is of particular interest with respect to understanding organic species' reactivity on metal surfaces and use in catalytic systems.[2]

Unsaturated trinuclear metal complexes from group 9 metals, cobalt, rhodium, and iridium, are unusual and exhibit interesting properties because they are composed of electon-rich metals in an electron deficient environment. The extremely reactive, 46 electron, trinuclear cobalt cluster containing the π-acid ligand, CO, is one of the most unique in the series.[3] Although the synthesis of the trinuclear **1** has been extensively developed and tested, several questions regarding its magnetic properties remain.[4] In 1989 Barnes and Orvis reported that temperature dependent magnetic susceptibility studies indicated that trinuclear **1** exhibited paramagnetic properties above 100K and diamagnetic properties below 100K.[4] The

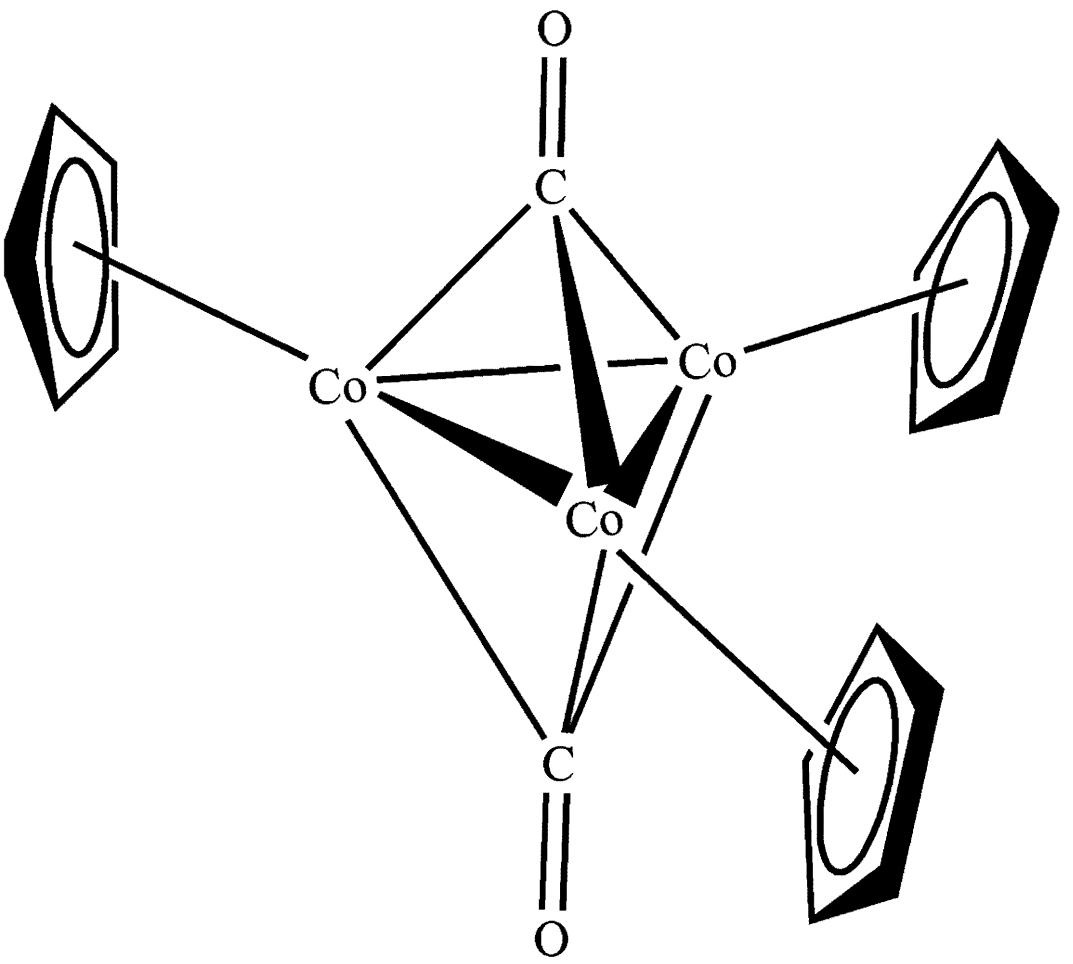

Figure 1.1. $(CpCo)_3(CO)_2$ structure, which will be the focus of Chapter II and will be abbreviated as trinuclear **1** throughout this work.

intent of this thesis is to gain a better understanding of the temperature dependent change in crystal structure that occurs in the Co_3 cluster through X-ray crystallography studies at various temperatures.

In order to perform X-ray crystallography studies on the Co_3 cluster a special device for mounting the crystals on the goniometer head was constructed. Using diagrams from Sauer and Ceska's 1997 publication,[5] a pin consisting of a capillary, fiber loop, and copper pin was created so that the small, thin plate crystals could be easily mounted into the X-ray beam without breaking or cracking. There are several advantages to this capillary-fiber method of crystal mounting including less unwanted interference by amorphous material in the diffraction pattern. These advantages will be discussed further in Chapter II.

The synthesis of zirconium halide clusters has long been known; however, their stability in solution is a new discovery. It was not until 1999 that Xie and Hughbanks reported $[Zr_6CCl_{12}Cl_6]^{4-}$ and $[Zr_6BCl_{12}Cl_6]^{5-}$ were both soluble and stable in water and methanol.[6] It was previously assumed that solid state clusters would undergo oxidation and solvolysis in the presence of water due to their low oxidation state of +3; however, this proved to be false. The stability of clusters in solution, especially aqueous media, has opened new doors for cluster chemistry.

$[Zr_6BCl_{12}]^+$ cluster-based crystals were synthesized and analyzed by Xie, Reibenspies, and Hughbanks in 1998.[7] In 1999 $[Zr_6BBr_{12}]^+$ crystals were synthesized and characterized by Xie and Hughbanks.[8] This left only the synthesis of the $[Zr_6BI_{12}]^+$ crystals to complete the halide family. Chapter III presents the synthesis and characterization of the iodide analogue and includes a comparative look at the structural trends in the halide family of hexazirconium halide cluster complexes.

CHAPTER II

$(Co(\eta^5\text{-}C_5H_5))_3(CO)_2$: Synthesis and Temperature Dependent Structural Study

The Co_3 cluster is formed by the reaction of two mole equivalents of η^5-Cyclopentadienylbis(ethylene)cobalt(I) ($Co(\eta^5\text{-}C_5H_5)(C_2H_4)_2$), $CpCo(C_2H_4)_2$, with η^5-Cyclopentadienyl cobalt(I) dicarbonyl ($Co(\eta^5\text{-}C_5H_5)(CO)_2$), $CpCo_3(CO)_2$ in a hexane / ether solvent. The trinuclear product is produced via a step-wise process. The lability of the ethylene ligands allows the molecule to function as a CpCo fragment synthetically, which is added to the $CpCo(CO)_2$ to form the dinuclear complex $[Co(\eta^5\text{-}C_5H_5)(\mu\text{-}CO)]_2$. A second CpCo fragment adds to one face of the dinuclear complex forming the desired trinuclear product. For a depiction of this reaction sequence see Figure 2.1.

Techniques: Handling of air-sensitive compounds

The step-by-step procedure for the synthesis of the Co_3 complex has been documented in detail by Barnes and Orvis.[4] Since many of the reactants and products in the multistep synthesis are extremely air and moisture sensitive much of the work was conducted in an inert atmosphere dry box using Schlenk techniques.

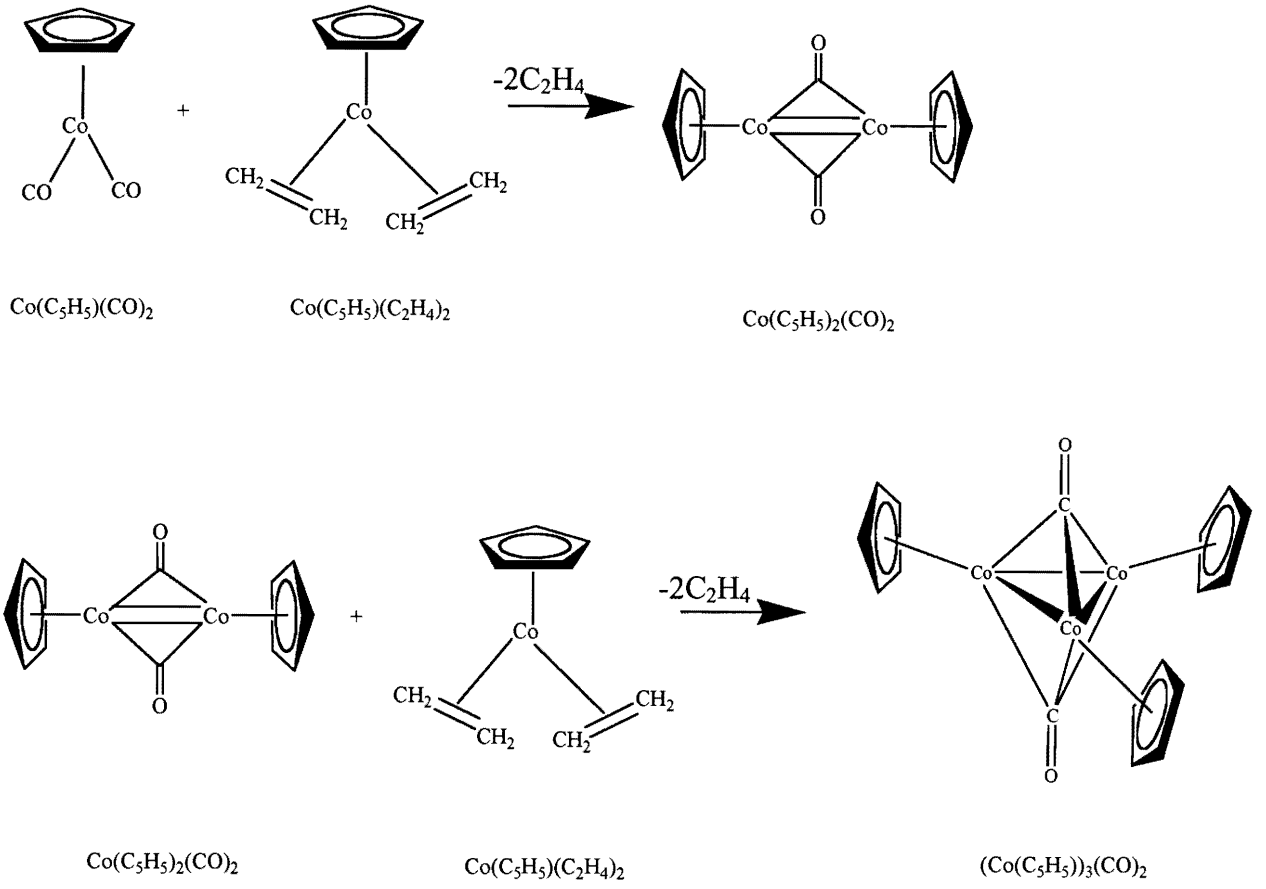

Figure 2.1: Addition of CpCo fragments to form the Co_3 cluster.

Synthesis: $(Co(\eta^5\text{-}C_5H_5))_3(CO)_2$

Hexaaminecobalt (II) chloride, $[Co(NH_3)_6]Cl_2$.

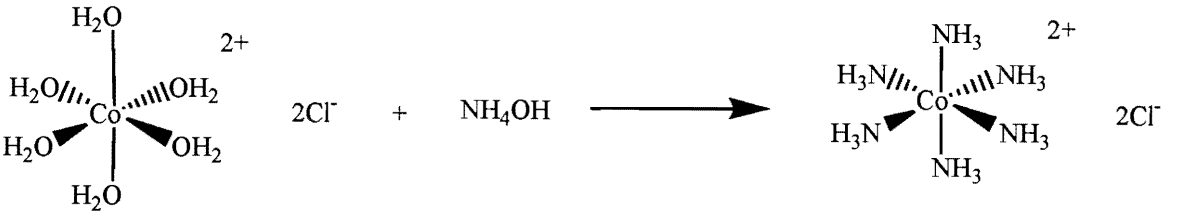

$[Co(H_2O)_6]Cl_2$ $[Co(NH_3)_6]Cl_2$

26.602g of Cobalt (II) chloride hexahydrate (0.112moles, $Co(H_2O)_6Cl_2$) was ground into a powder and placed in a 500mL Schlenk vessel. 200mL of aqueous ammonia were added to the vessel. The solution became a dark red-brown. While stirring, the solution was heated to just below the boiling point for one and a half-hours. Upon completion of the reaction, a pink-peach precipitate was noticed suspended in the dark red-brown solution. The solution was allowed to cool to room temperature and then stored at 5°C overnight. The following day the solution was found to have lightened in color to a dark red and the quantity of the pink-peach precipitate had increased. The Schlenk vessel was submerged in an ice bath to prevent the solid from redissolving. The precipitate was then isolated by canulation. The solid was washed twice with 200mL portions of degassed methanol and one final wash with 200mL ether. On a standard vacuum line, the solid was dried for one hour leaving a light, fluffy pink solid. The yield was 16.6155g $Co(NH_3)_6Cl_2$ (0.0716moles, 62.46%). The air and moisture sensitive solid was stored in an inert atmosphere dry box.

Cyclopentadiene, C_5H_6. Several of the following synthesis steps require the use of cyclopentadiene, which exists as the dimer dicyclopentadiene at room temperature. In order to

"crack" the dimer 500mL of dicyclopentadiene were placed in a 1000mL round bottom flask with a small amount of iron shavings. The round bottom was fitted with a distillation column and a condenser. The collecting Schlenk vessel was placed in a Dewar containing a mixture of 2-isopropanol and dry ice (-70°C). The round bottom flask was heated for five hours and the fraction that distilled at 45-50°C was collected. The cyclopentadiene was stored under nitrogen at -70°C and used as needed.

Sodium Cyclopentadienide, NaC_5H_5.

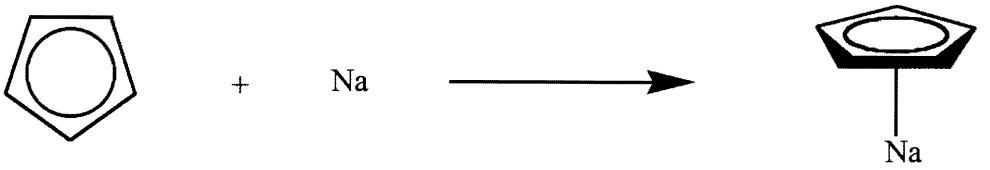

C_5H_6 NaC_5H_5

To maximize surface area and therefore reactivity, sodium sand was produced by warming and vigorously stirring 25g (1.09moles) of sodium metal in a 1000mL round-bottom flask containing 300mL of freshly distilled toluene. Once the sodium was molten, the heat was removed and as the small beads were allowed to solidify. While under nitrogen flow, the toluene was decanted. 250mL of freshly distilled tetrahydrofuran were added to the flask. The flask was submerged in an ice bath and 75mL (1.13moles) of freshly cracked cyclopentadiene (C_5H_6) was added in 3mL portions while stirring vigorously. The reaction was stirred overnight under nitrogen allowing it to reach thermal equilibrium. The following morning the solution had become a pink-red-brown color. The solution was canulated into a fresh Schlenk vessel in order to separate it from the excess sodium. The solvent was removed on a vacuum line and the

remaining beige solid was dried on a diffusion pump vacuum line. 75.352g of sodium cyclopentadienide (0.855moles, NaC_5H_5) were produced. The percent yield, based on the amount of cyclopentadiene was 70.36%. The air sensitive compound was stored in an inert atmosphere dry box.

The above reaction evolves hydrogen gas and should be completed in a well-ventilated hood. It should also be noted that both sodium and sodium cyclopentadienide react violently in air; therefore, extreme caution should be used when removing compounds from the dry box.

Bis(η^5-cyclopentadienyl)cobalt(II), Cobaltocene, Co(η^5-C_5H_5)$_2$.

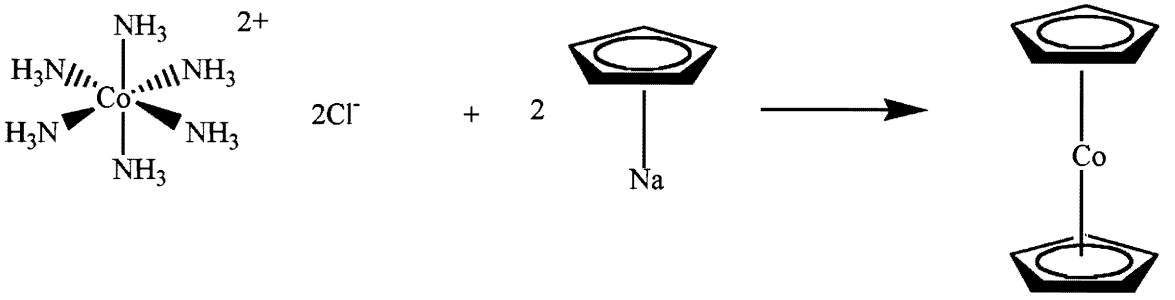

$[Co(NH_3)_6]Cl_2$ $Na(C_5H_5)$ $Co(C_5H_5)_2$

16.372g of hexaaminecobalt (II) chloride (0.071moles, $[Co(NH_3)_6]Cl_2$) and 18.555g of sodium cyclopentadienide (0.211moles, NaC_5H_5) were weighed out in an inert atmosphere dry box and placed in a 500mL Schlenk vessel. The Schlenk vessel was removed from the dry box and degassed and refilled with nitrogen. 100mL of freshly distilled tetrahydrofuran were added to the Schlenk while under nitrogen purge. The solution became dark red-brown and began to bubble releasing ammonia. The solution was refluxed for two hours. The solvent was then removed under vacuum. The dark gray-purple solid was stored under nitrogen overnight. To purify the product, a sublimation was performed. In the inert atmosphere dry box the solid was

transferred to a 150mL round-bottom flask. A layer of glass wool was placed over the cobaltocene containing powder and a condenser was attached to the round bottom. The apparatus was removed from the dry box and connected to a diffusion pump vacuum line. The round bottom flask was heated to 75°C using a silicon oil bath and left overnight. The following day, beautiful, purple-black crystals had formed in the condenser. The apparatus was taken back into the inert atmosphere dry box and the crystals were placed in a new vessel. The yield was 73.32% corresponding to 9.785g (0.052moles) of cobaltocene. The crystals were stored under nitrogen in the freezer at -20°C until needed.

Ammonia gas is evolved in this reaction and therefore the reaction should be attempted only in a well-ventilated hood.

η^5-Cyclopentadienylbis(ethylene)cobalt(I), $Co(\eta^5\text{-}C_5H_5)(C_2H_4)_2$.

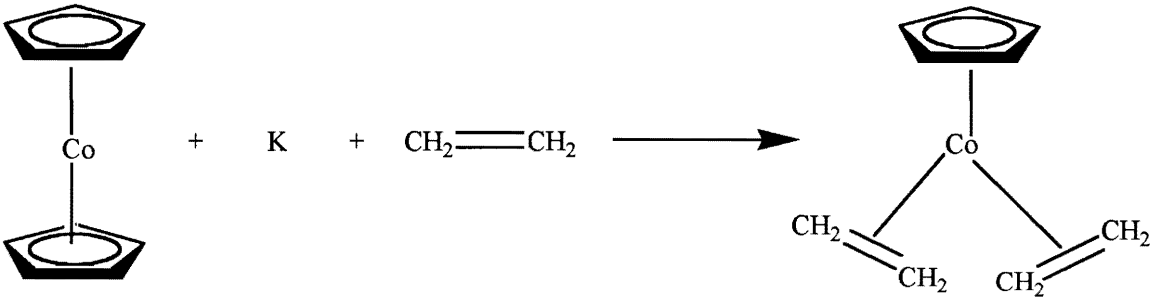

$Co(C_5H_5)_2$ $Co(C_5H_5)(C_2H_4)_2$

In an inert atmosphere dry box 4.990g of ground cobtaltocene powder (0.027moles, $Co(\eta^5\text{-}C_5H_5)_2$) were added to a jacketed Schlenk vessel. While under an ethylene overpressure 400mL of degassed ether was added to the jacketed Schlenk vessel. Using a circulating cooler, the reaction vessel was cooled to -10°C for the entire duration of the reaction. The solution was placed under a slight ethylene overpressure, stirred, and 0.75g portions of freshly shaved

potassium metal were added twice daily. Over a six-day period the solution changed from a dark red to an orange-red to an orange-brown color. After six days of adding potassium metal, the solution was allowed to settle revealing a deep red-orange-brown layer, the desired cyclopentadienylbis(ethylene)cobalt(I) ($Co(\eta^5\text{-}C_5H_5)(C_2H_4)_2$) product and a gray layer, potassium cyclopentadienide (KC_5H_5). The red-orange-brown layer was canulated into a Schlenk vessel at -70°C. Using a vacuum line, the solvent was removed until approximately 10mL of solution remained. 250mL of degassed, freshly distilled hexane were added to the solution. The solution was then filtered to remove any solid particles. The hexane was removed under vacuum leaving an orange precipitate, which was stored under nitrogen in the freezer at -20°C until needed. The reaction yield was quite low, which was perhaps due to allowing the reaction to run longer than necessary.

Due to the involvement of ethylene gas in the reaction, all procedures should be attempted in a well-ventilated hood. Additional precautions include the threat of the solution becoming supersaturated with ethylene and boiling out when the stopper is removed to add potassium.

η^5-Cyclopentadienyl Cobalt (I) Dicarbonyl, $Co(\eta^5\text{-}C_5H_5)(CO)_2$.

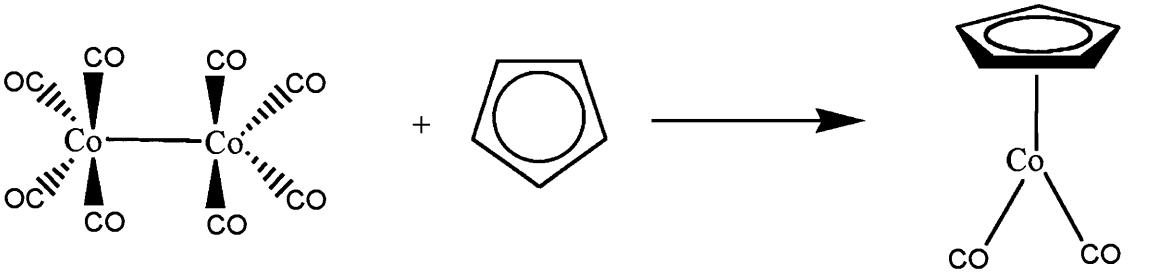

$Co_2(CO)_8$ C_5H_6 $Co(C_5H_5)(CO)_2$

10.1g of dicobalt octacarbonyl (0.030moles, $Co_2(CO)_8$) were placed in a Schlenk vessel. Under nitrogen purge 200mL of distilled methylene chloride (CH_2Cl_2) were added to the vessel. The solution was warmed to dissolve the dicobalt octacarbonyl ($Co_2(CO)_8$) at which time it became dark brown in color. While stirring, 2.0mL of freshly cracked cyclopentadiene (C_5H_6) were added to the solution. A reflux apparatus was attached to the vessel and the heat was increased until the solution reached a stable reflux. The solution was allowed to reflux overnight. The following day, the solution was still very dark, but had a deep red color in transmitted light. The solvent was removed under vacuum until approximately 8mL of a thick, oily solution remained. The thick solution was then distilled using a microdistillation apparatus. First, the remaining methylene chloride was removed. Afterward, a yellow-orange oil began to distill, the Schlenk vessel was changed to collect the end product, $Co(\eta^5\text{-}C_5H_5)(CO)_2$. The yield of the $Co(\eta^5\text{-}C_5H_5)(CO)_2$ was well below 30% because the product began to distill while the methylene chloride solvent was still being removed.

^1H NMR (C_6D_6): δ 4.39ppm.

Tri η^5-Cyclopentadienyl Tricobalt (I) Dicarbonyl.

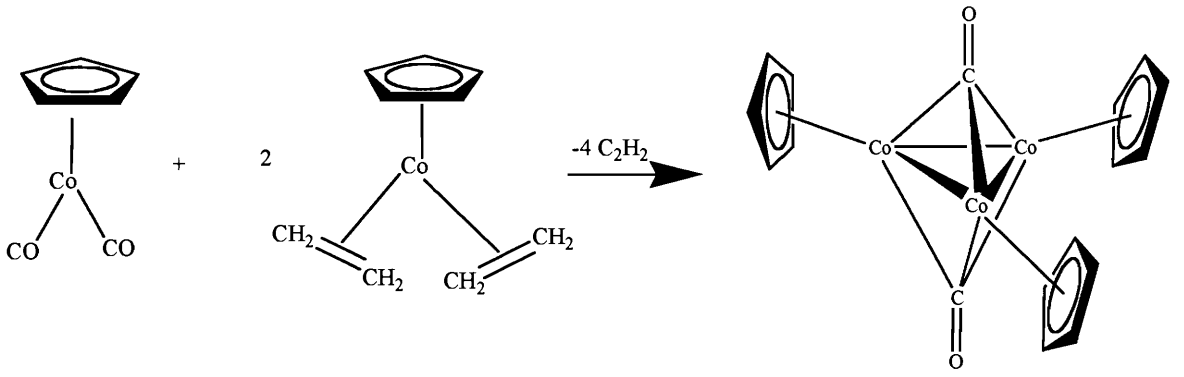

$Co(C_5H_5)(CO)_2$ $Co(C_5H_5)(C_2H_4)_2$ $(Co(C_5H_5))_3(CO)_2$

In an inert atmosphere dry box, 50mg (0.3 mmoles) of $CpCo(CO)_2$ were dissolved in ether. The solution was filtered through a pipet with cotton into a 500mL Schlenk vessel. 50mg of $CpCo(C_2H_5)_2$ (0.6 mmoles) were dissolved in hexane and the solution was filtered into the Schlenk vessel containing the $CpCo(CO)_2$ / ether solution. The solution immediately turned a dark green and small black crystals began to precipitate. The Schlenk vessel was removed from the dry box and the solvent was decanted. The remaining crystals were washed with freshly distilled hexane until the supernanate was virtually colorless. The crystals were dried on a standard vacuum line and stored under nitrogen at -5°C until needed. The synthesis yielded a mixture of crystals with included irregular shapes and some possessing a perfect hexagonal shape. The black plates had an average size of 0.2 x 0.2 x 0.01 mm.

^1H NMR (C_6D_6): δ -32.06ppm

Structural Analysis: Temperature dependent structural change in single crystal $(CoCp)_3(CO)_2$

In 1989, Barnes and Orvis used NMR techniques to determine that trinuclear **1** exhibited paramagnetic character at room temperature.[4] Using the Evans' NMR method for determining magnetic moments the origin of the paramagnetism of the trinuclear **1** was determined to be from perhaps a triplet spin state. However, further studies of the magnetic properties in the solid state indicated that at temperatures below -150°C the cluster loses its paramagnetism; therefore, trinuclear **1** is not a ground state triplet molecule. The source of the change in magnetism was not determined but was hypothesized to be a structural change in the molecule.

In an attempt to determine the source of the change in magnetic properties of the trinuclear **1** a temperature dependent X-ray diffraction study was conducted. Due to the fragility of the thin, plate crystals a special mounting method was devised to place the crystal on the goniometer head. Adapting methods suggested by Sauer and Ceska's 1997 publication,[5] a small fiber was threaded into a pulled glass capillary to form a loop. The loop was then used to gently "catch" the plate crystal while suspended in paratone oil. The initial step in constructing the loops was to warm and pull glass microcapillaries to an approximate diameter of 0.4mm. One end of a strand of human hair was the threaded into the tip of the capillary. To form a loop, the second end of the hair was threaded into the capillary and pulled until the desired diameter of 0.3mm was reached. The hair was then secured by epoxy glue. To prevent cracking of the glue and in turn loosening of the loop while under low temperatures the epoxy was used in two parts polymer to one part hardener ratio. The capillary and attached loop were then trimmed to approximately 2.5cm in length and attached to a hollow copper goniometer pin using 1:1 epoxy. In order to reduce the opportunity for ice buildup on the goniometer pin during low temperature studies care was taken to make rounded tips at all connection points. Once the crystals are suspended in paratone oil they can easily be mounted on the goniometer with reduced risk of fracture and breakage by gently sliding the fiber loop underneath the crystal and slowly scooping it up from the paratone oil. Figure 2.2 depicts the procedure used for constructing capillary loop pins.

There are two primary advantages of using the capillary loop method for mounting crystals. The first being the ease with which fragile crystals such as thin plates can be mounted and the second, the reduction of interference of the x-ray beam by amorphous material such as a glass pin.

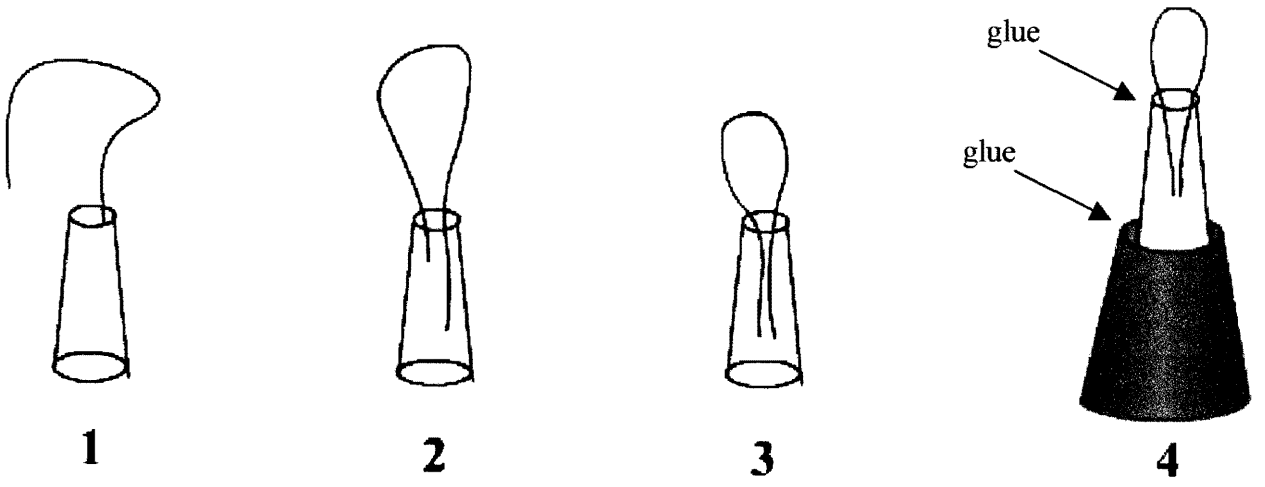

Figure 2.2. Using capillary tube and fiber methods similar to that reported by Sauer and Ceska in 1997[5] pins were constructed for mounting the fragile plate crystals.

1) A human hair was inserted into the pulled glass capillary
2) The second end of the hair was threaded into the capillary to form a loop
3) To make the loop the desired diameter one end of the fiber was pulled. The fiber was then secured to the glass capillary using 2:1 Epoxy
4) The glass pin was attached to a copper goniometer pin using Epoxy glue.

Since the crystal is located inside (or preferable on the tip of) a loop, which is extended 0.4mm from the glass capillary the beam of X-rays is less likely contact the glass and copper pins, thereby reducing the scattering from amorphous material.

Using a Siemans (Bruker) Smart 1000 CCD X-ray diffractometer the single crystal structure of Co_3 was determined at seven temperatures ranging from -75°C to -157°C. The diffractometer was equipped with an LT-3 low temperature apparatus, which provided a stream of dry nitrogen on the crystal at the desired temperature. The single crystal was mounted using the capillary loop method previously described. Each of the seven data sets was collected under identical conditions. A hemisphere of data was collected using an omega scan of 0.3° per frame while integrating for 55 seconds per frame. The angle Phi was set to 0.0°, 120°, and 240° for runs 1, 2, and 3, respectively. The use of 120° and 240° rather than the default 90° and 180° is to prevent the measurement from occurring edge-on the thin plate. With a thickness of only 0.01mm it is undesirable to record diffraction measurements in the edge-on orientation. The crystal is mounted so that the main face is perpendicular to the x-ray beam at Phi = 0.0°. With Phi = 120° and 240° during ω (omega) rotations, edge-on measurements are avoided. 1265 frames of data were collected. The unit cell parameters of the crystal were obtained using SMART software and further refined using SAINT software. SADABS v2.01 was used to correct for absorption of the X-rays by the plate crystal. Face 001 was specified as the major face of the plate. The crystal structure was determined to be hexagonal and in the P6(3)/m space group. There were two molecules per until cell; Z = 2.

The molecule exhibits C_{3h} symmetry due to the orientation of the cyclopentadiene rings. A thermal ellipsoid drawing of the Co_3 crystal structure can be seen in Figure 2.3.

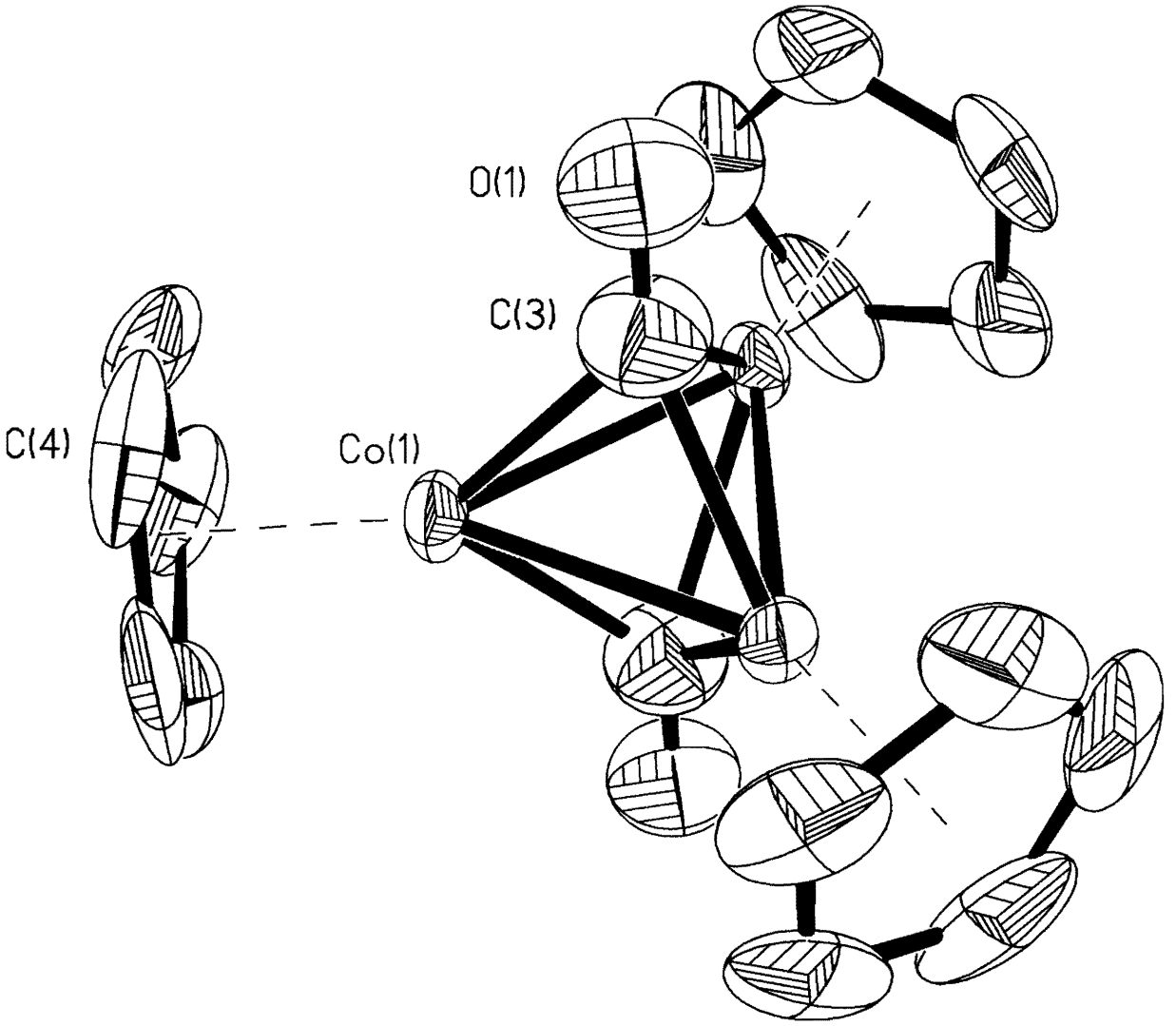

Figure 2.3. A thermal ellipsoid drawing of Co_3.

The molecule has two symmetry elements, a three-fold rotational axis along the carbonyl bond and a mirror plane perpendicular to the rotational axis. Due to the three-fold symmetry there are only eight unique atoms in the molecule, one cobalt, three carbons and 3 hydrogens, which compose the cyclopentadiene rings, and one carbon and oxygen, which form the carbonyl groups. The molecule is oriented in the unit cell with the Co—Co bonds in the *a*-b plane and the carbonyl ligands oriented along the *c* axis, which can be seen in the unit cell packing diagram, Figure 2.4.

The unit cell parameters *a, b,* and *c* and the bond lengths were found to vary with temperature. The average Co—Co bond length in the -75° to -157°C temperature range was 2.341(1)Å, while the average Co—C = O bond length was 1.963(9)Å and the average Co—Cp bond distance was 2.071(7)Å.

Figure 2.5 illustrates the change in unit cell parameters with respect to temperature. Notice that unit cell parameters *a* and *b* display a large change in length in the temperature range of -90° to -120°C, while unit cell parameter *c* does not. The decrease in unit cell parameters *a* and *b* dictate a shortening of the Co—Co bond lengths because they reside in the same plane. Figures 2.6 and 2.7 are identical to Figure 2.5, but illustrate different orientations of **1** with respect to *a, b,* and *c*.

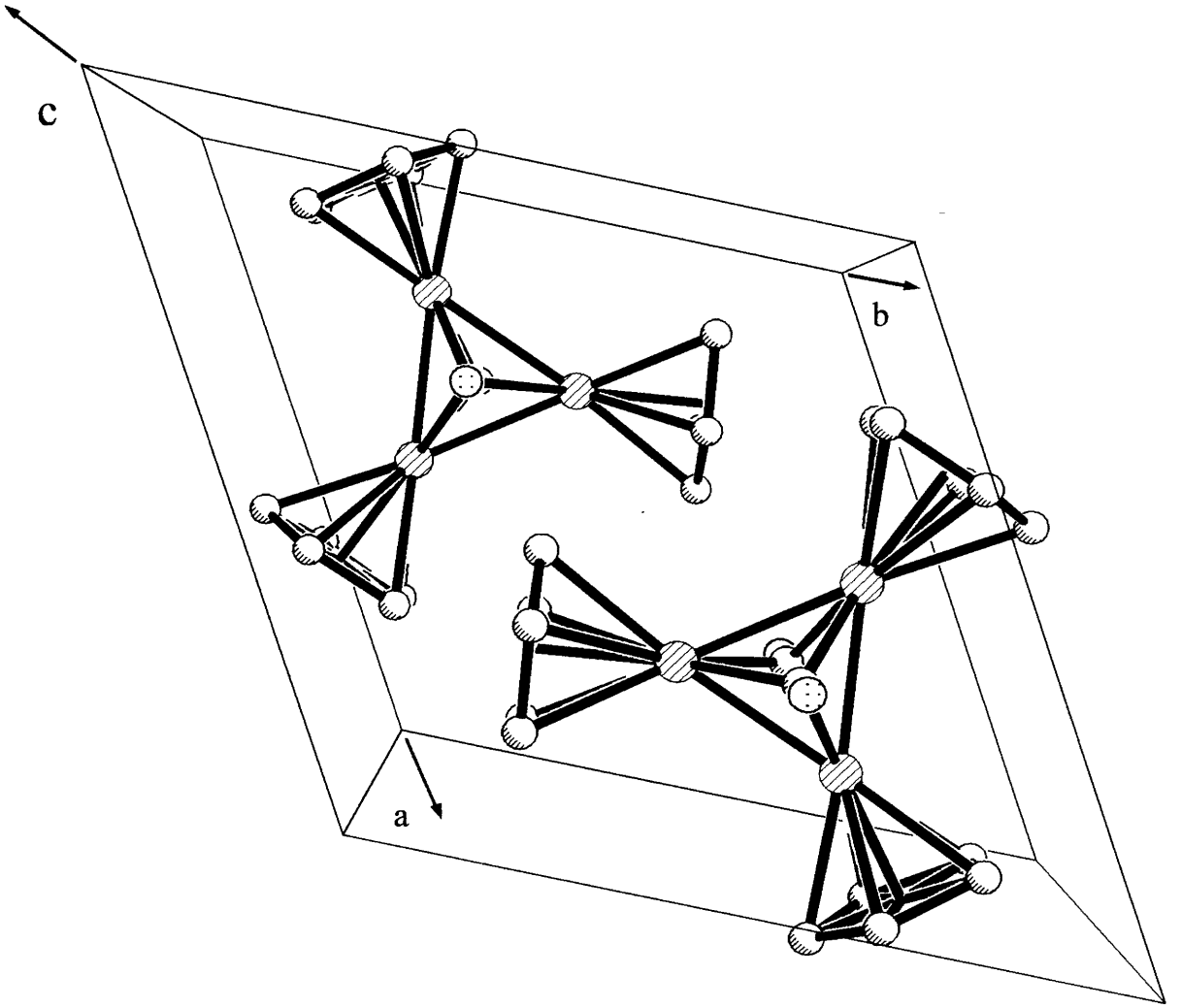

Figure 2.4. A unit cell packing diagram of Co_3. Notice there are two clusters per unit cell, Z=2.

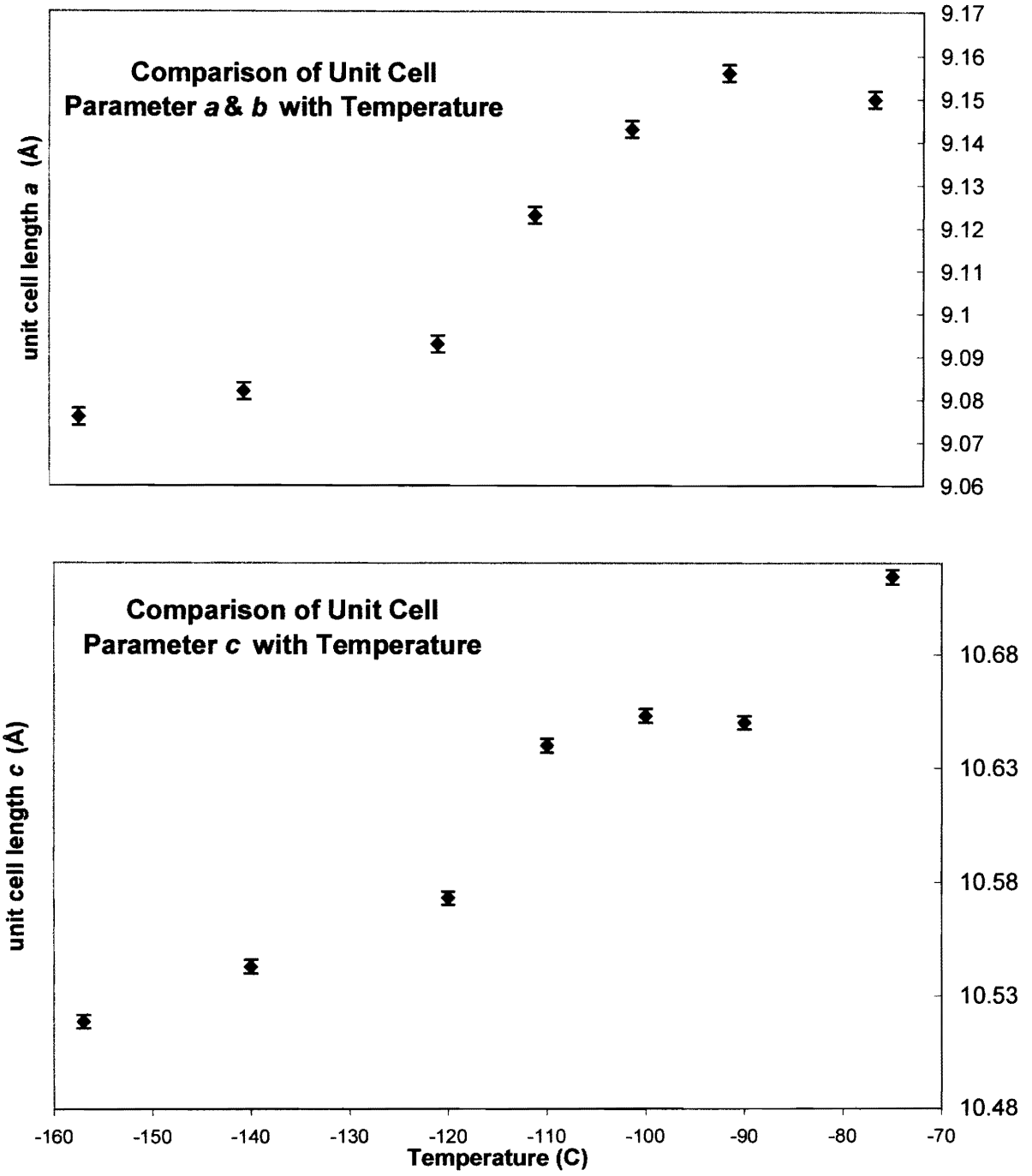

Figure 2.5. A comparison of unit cell parameters with temperature. Parameters *a* and *b* experience a sharp decrease in length in the -90° to -120°C that parameter *c* does not. Error bars represent three times the estimated standard deviation in the length.

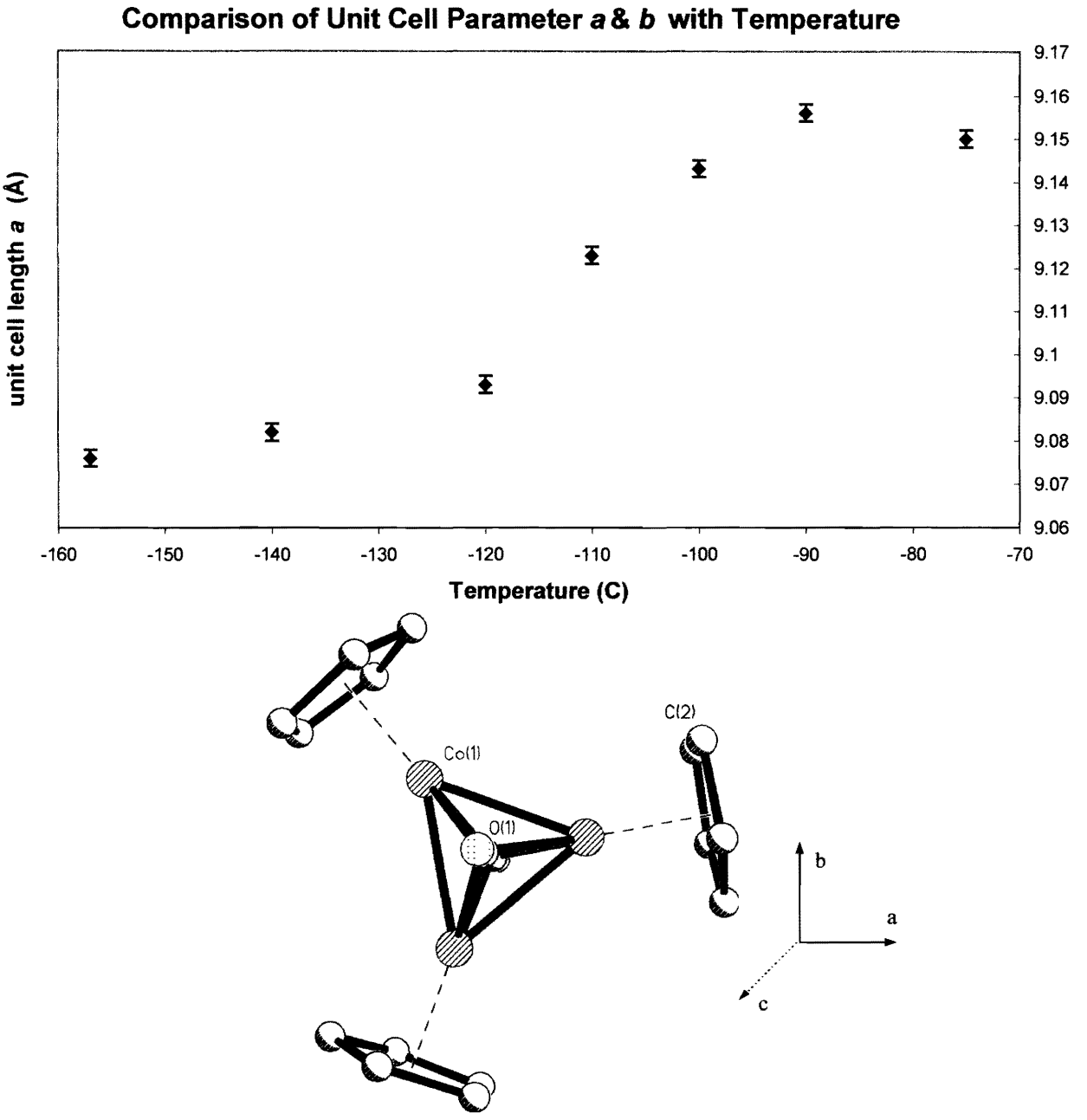

Figure 2.6. Tricobalt plane is rigorously located in the *a-b* plane of the unit cell. Error bars represent three times the estimated standard deviation in the length.

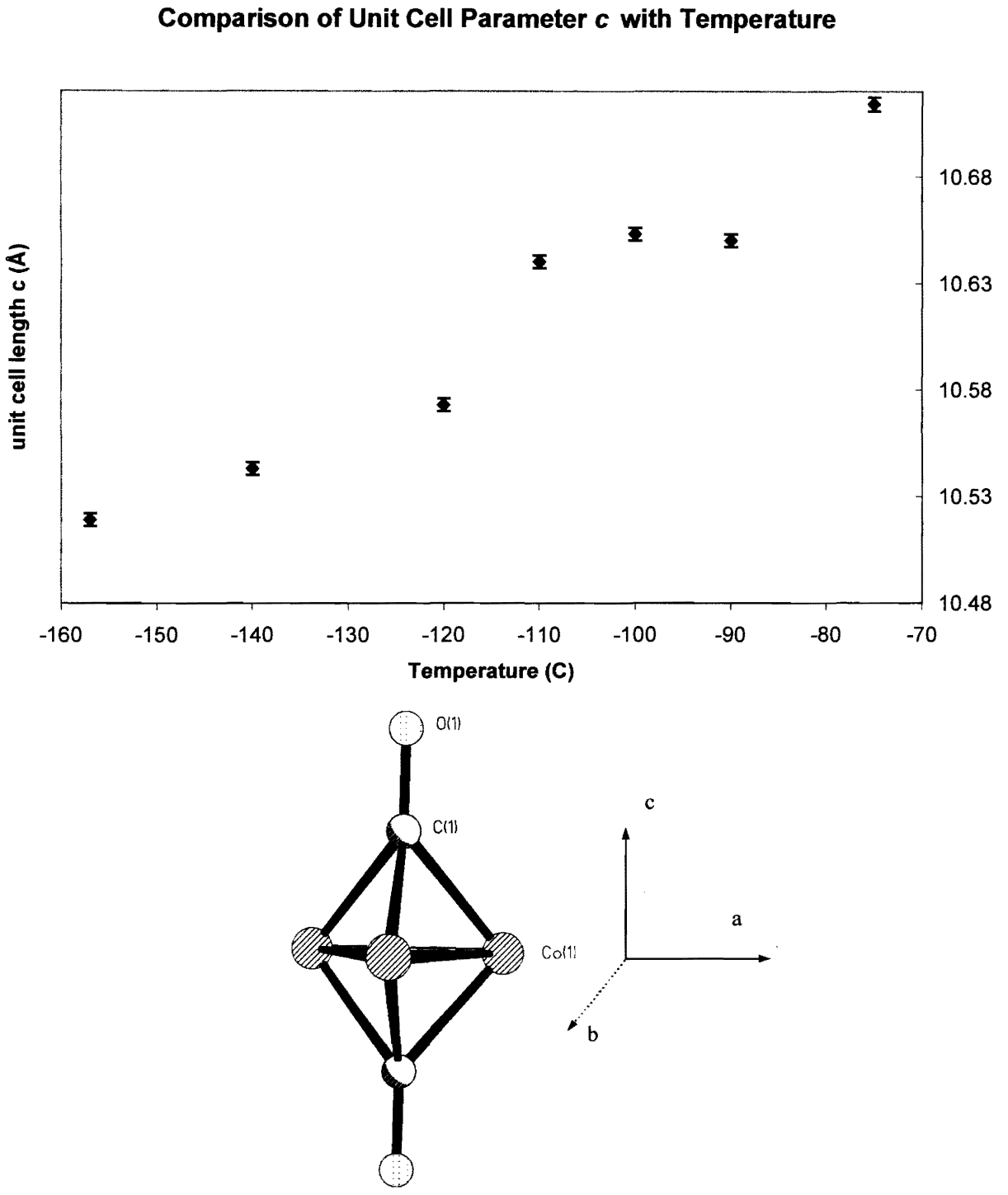

Figure 2.7. The carbonyl bonds are along the *c* unit cell axis. Error bars represent three times the estimated standard deviation in the length.

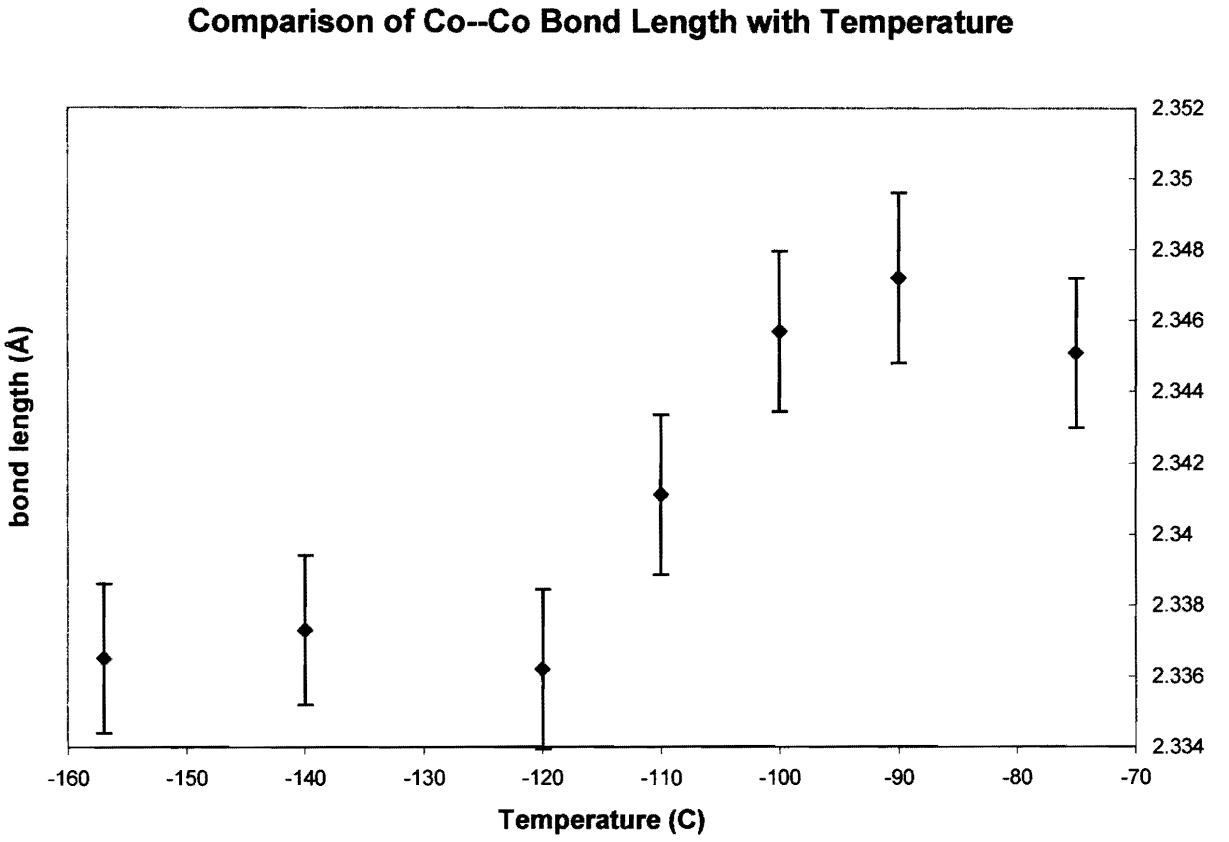

Figure 2.8. Co—Co bond lengths in the -75° to -157°C range. Error bars represent three times the estimated standard deviation in the length.

Table 2.1. Change in Unit Cell Parameters with Temperature for Co_3

Temperature (°C)	[a]Unit Cell Parameter *a* (Å)	[a]Unit Cell Parameter *c* (Å)	[a]Co—Co Bond Length (Å)	[a]Co—C Bond Length (Å)
-75	9.150(1)	10.714(2)	2.344(1)	1.965(9)
-90	9.156(1)	10.650(2)	2.347(2)	1.95(1)
-100	9.143(1)	10.653(2)	2.346(1)	1.963(9)
-110	9.123(1)	10.640(2)	2.341(1)	1.967(8)
-120	9.093(1)	10.573(2)	2.336(1)	1.965(9)
-140	9.082(1)	10.543(2)	2.337(1)	1.957(8)
-157	9.076(1)	10.519(2)	2.337(1)	1.967(8)

(a) Numbers in parentheses represent one standard deviation in the last significant figure in the bond length

Knowing that a change occurs in the Co—Co bond distances, a closer look was taken at Pinhas's 1980 Helvetica Chemica Acta article entitled, "A Class of Trinuclear Clusters with Carbonyl Bridging",[11] which depicts a theoretical calculation of the molecular orbitals for the rhodium analogue of **1**, $(RhCp)_3(CO)_2$. The origin of the highest occupied molecular orbital, HOMO, is depicted in Figure 2.9. The degenerate HOMO is formed by three out of plane cobalt d-orbitals together with the carbonyl π^* orbitals. Unfortunately, the underlying cause of the magnetic phase change is not obvious from these results; however, further studies will be conducted to relate the magnetic phase change to the compounds electronic structure.

Future Studies

In an attempt to determine the origin of the magnetic phase change in trinuclear **1** a closer look will be taken at the shape of the carbon thermal ellipsoids of the cyclopentadiene rings. Theoretical studies of the electronic structure of compound **1** will also be considered.

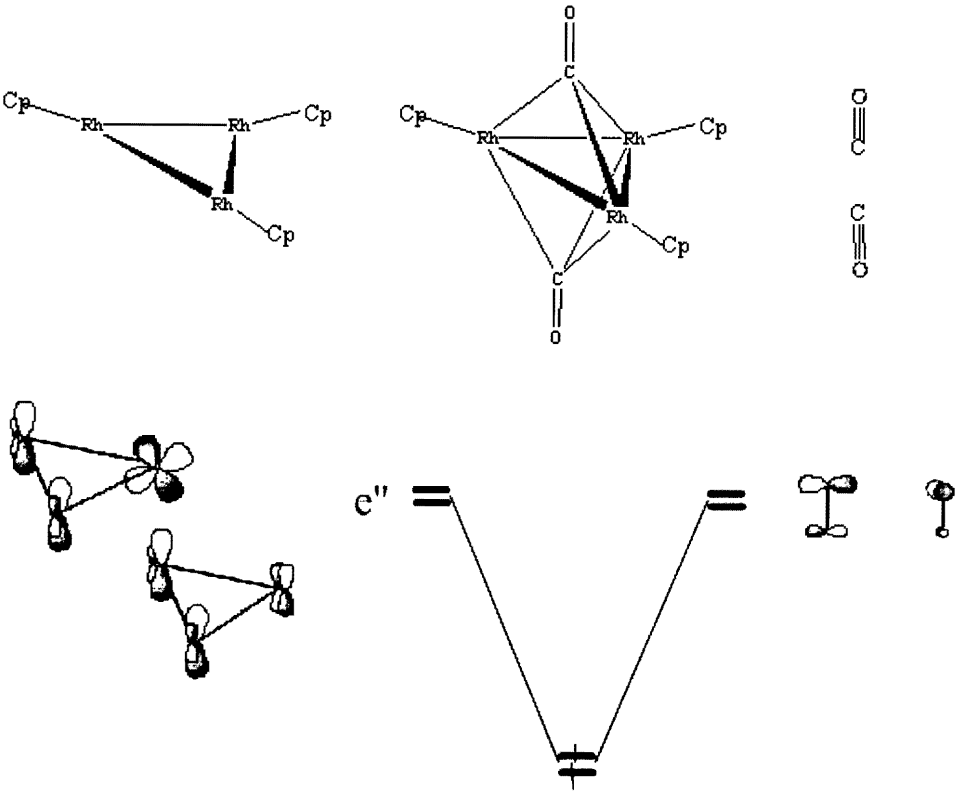

Figure 2.9. The HOMO for $(RhCp)_3(CO)_2$. This diagram was recreated from Pinhas' 1980 article from *Helvetica Chimica Acta*.[11]

CHAPTER III

$[Zr_6I_{12}(CH_3OH)_6][I(CH_3OH)_6]$: Synthesis and Characterization

Solid-state hexazirconium halide clusters have a general composition of $M_y[(Zr_6ZX_{12})]X_q$, where M is an alkali or an alkaline earth metal cation, Z is an interstitial atom, and X is a halide. The connectivity of the clusters is determined by the values of y and q, which have been found to range from 0 to 6. Hexazirconium chlorides have been found with compositions ranging from $Zr_6Cl_{12}B$ to $Zr_6Cl_{18}B$. However, to date, iodide clusters have only been found to exist as 6-12 and 6-14 stoichiometry.[9]

Two examples of the cluster connectivity that occurs are illustrated in Figures 3.1 and 3.2. Figure 3.1 is a depiction of cluster compounds with 6-18 composition, which are present as single unit structures with each cluster existing independently, i.e. no halogen bridging. Compounds with stoichiometry less than 6-18 form bridges across the halogen atoms.[10] In Figure 3.2, notice that $\mathbf{I}^{a\text{-}a}$ is a halide bridge formed by a terminal bond to two metal clusters, which is noted as *a-a* or ausser-ausser bridging. $\mathbf{I}^{i\text{-}a}$ depicts the halide atom forming an inner bridge with one cluster and a terminal bridge with the second, indicated by *i-a* or inner-ausser. This bonding pattern is characteristic of fourteen electron, 6-14 clusters. Bonding patterns vary for other stoichiometries and cluster based electron counts. The network structure within solid-state clusters is important and impacts their ability to be excised.

Xie and Hughbanks' 1999 discovery of the stability of reduced hexazirconium clusters in aqueous media has bridged the way for the substitution of cluster ligands and the production of more soluble polycrystalline materials.

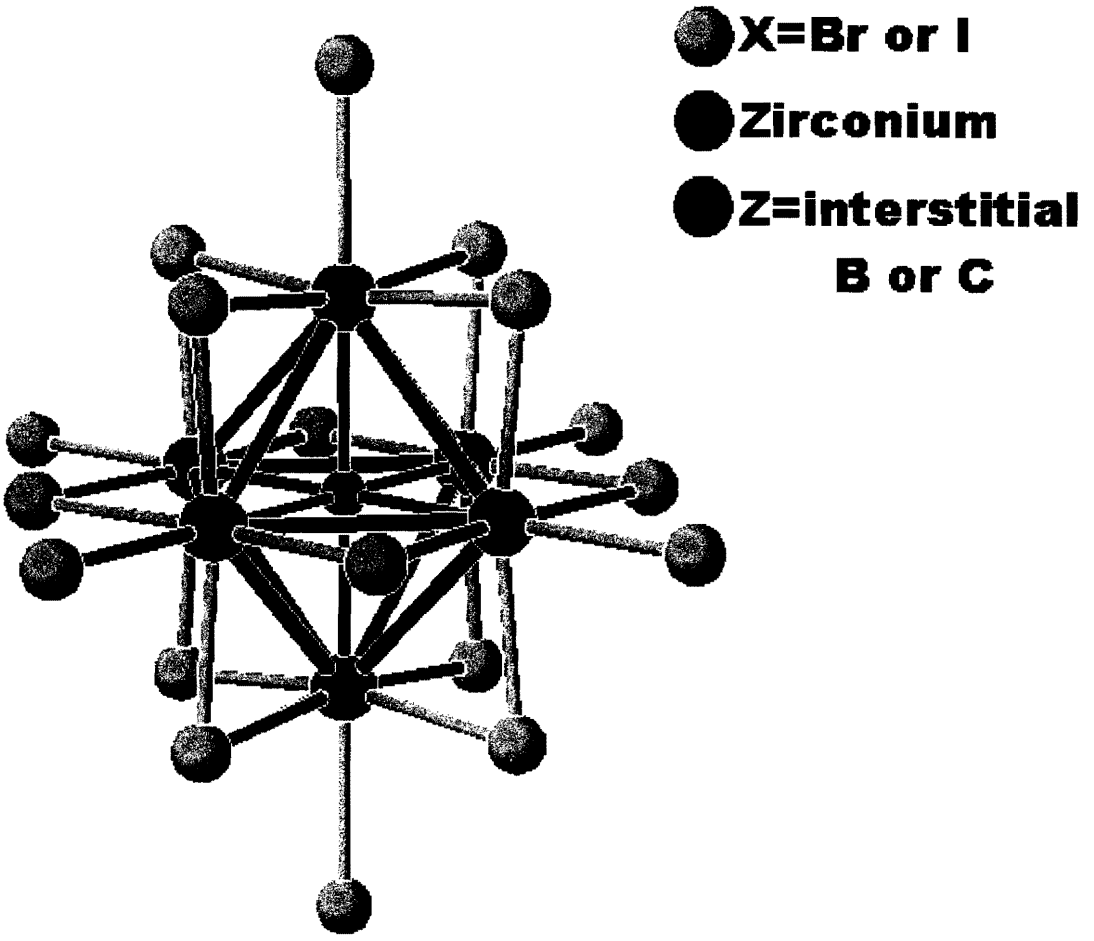

Figure 3.1: Solid-state building block with $[Zr_6X_{18}Z]$ stoichiometry.

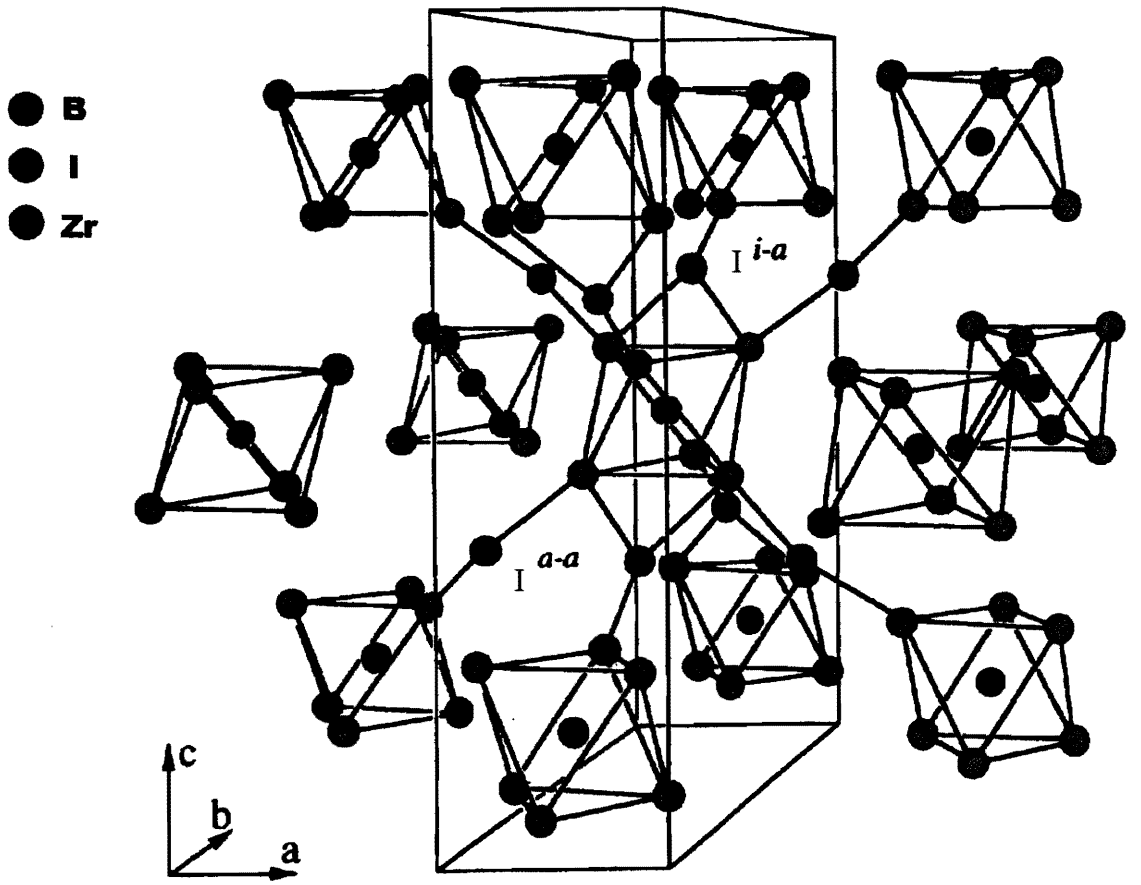

Figure 3.2: $[Zr_6I_{14}B]^+$ structure demonstrating the bridging between cluster molecules. The bridging labeled I^{a-a} indicates ausser-ausser bridging, while I^{i-a} is an example of inner-ausser bridging. (Figure taken from Cotton, F. A.; Hughbanks, T.; Runyan, C. E.; Wojtczak, W. A.; "Halide-Supported Octahedral Clusters of Zirconium: Structural and Bonding Questions", *Early Transition Metal Clusters with π-Donor Ligands*, 1-26(1995).

Techniques: Methods for Handling Air Sensitive Compounds

Due to the air sensitivity of the reactants and the products all experimentation was conducted using a combination of a standard high vacuum line, an inert atmosphere dry box, and Schlenk techniques. All glassware was dried in an oven overnight before use. Solutions and reagents were manipulated using needles and syringes, which were first flushed with argon. The solutions were transported and stored in Pyrex tubes, which were sealed under vacuum.

Synthetic Procedure: $KZr_6I_{12}B$

$$KI + \frac{13}{4}ZrI_4 + \frac{11}{4}Zr + B \xrightarrow{850°C} KZr_6I_{14}B$$

Boron-centered hexazirconium iodide cluster, $KZr_6I_{12}B$.

Potassium iodide was vacuum sublimed and the zirconium powder was prepared by hydrogenation-dehydrogenation of Zr-foil. Aqueous solvents were deoxygenated by bubbling nitrogen gas through them for one day. The cluster compound was synthesized by heating the reactants in a niobium tube for two weeks. Niobium tubes were cut approximately two inches in length. The tubes were cleaned using a mixture of hydrofluoric acid and sulfuric acid and then dried overnight in an oven. One end was clamped closed using a vice. The closed end was then sealed with an argon arc welder. The niobium tubes were placed in the inert atmosphere dry box and stoichiometric amounts of potassium iodide, zirconium tetraiodide, zirconium powder, and boron powder were weighed out into the tube. Using vice grip pliers the other end of the niobium tube was carefully sealed to minimize exposure to air when transferred to the arc welder. The tubes were then placed in the arc welder and the second end sealed. Closing one

end of a 1.5inch diameter quartz tube created a quartz sleeve. The niobium tubes were then placed in the quartz sleeve and again washed with the sulfuric acid / hydrofluoric acid mixture. The open end was then closed around a 0.5inch neck, which was fitted for attachment to the vacuum line. The vessel was hung inverted for several hours to remove as much excess water as possible. The vessel was then placed on the vacuum line and lightly heated with a flame to evaporate any residual water. The quartz sleeve containing the niobium tubes was evacuated overnight and sealed the following morning. The sealed vessel was placed in a furnace, which was ramped up to 850°C and heated for two weeks. Figure 3.3 presents a depiction of the reaction apparatus. After the two-week heating period had passed the quartz vessel was removed from the furnace and quenched. The quartz sleeves were cut open and the niobium tubes taken into the inert atmosphere dry box. The tubes where then opened using serrated scissors and the contents were weighed. A yield of 90-95% was typically achieved.

In order to determine if the resultant product was indeed the KZr_6BI_{14} cluster, Guinier X-ray powder diffraction was used. The acquired Guinier X-ray diffraction patterns were compared with theoretical powder patterns generated by a FORTRAN IV program written by Clark, Smith, and Johnson. The synthesized product was found to be KZr_6BI_{14}.

Cluster Excision: Solution Chemistry of the $KZr_6I_{12}B$ cluster

In an inert atmosphere glove box the solubility of the $KZr_6I_{14}B$ cluster was tested in three deoxygenated solvents: methanol, pyridine, and water. The cluster was ground and 30-40mg was placed in an ampoule with a stirring bar. Three mililiters of deoxygenated solvent was added and the vessel was sealed under vacuum. The solutions were stirred for several days.

$$KI + \frac{13}{4}ZrI_4 + \frac{11}{4}Zr + B \xrightarrow{850°C} KZr_6I_{14}B$$

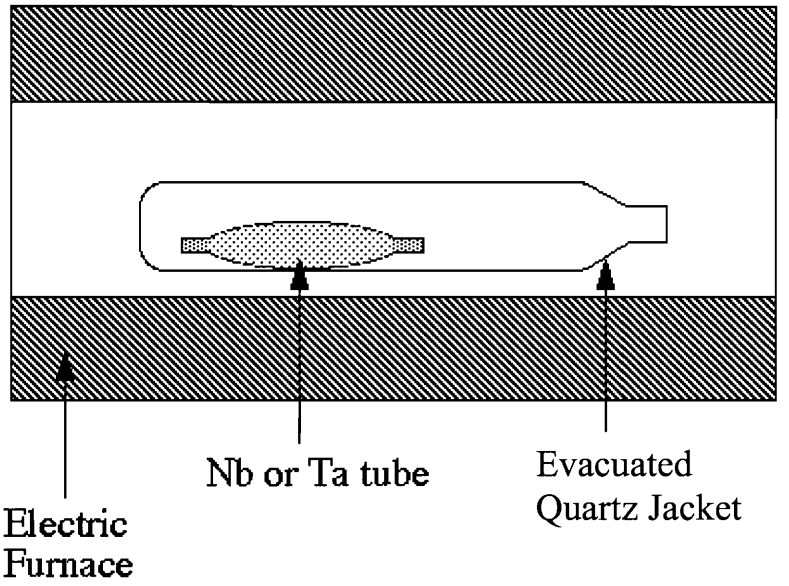

Figure 3.3. Depiction of apparatus used in the synthesis of $KZr_6I_{14}B$.

$KZr_6I_{14}B$ was found to be soluble only in water and this process was quite slow, taking up to one week to acquire an appreciable quantity of the cluster in solution. The solution was centrifuged and the supernanate was removed from the remaining solid. Additional water was added to the solid in an attempt to continue the excision. As the cluster was excised, the solution changed in color from green to deep red-brown. A color change in the solution typically indicates the presence of the cluster. A broad band ^{11}B NMR located a peak at 215ppm confirming that the cluster was intact in the solution.

In an attempt to substitute the iodide ligands and form a crystalline material, 3mL of 12M Hydrochloric acid was added to the aqueous $KZr_6I_{14}B$ solution in an inert atmosphere glove box and a brown polycrystalline material precipitated. To retrieve the solid the solution was decanted and the solid was dried in an inert atmosphere glove box. The polycrystals were determined to be soluble in methanol. The formation of the polycrystalline substance, which is thought to no longer possess a bridging halide network, allowed for the solubility of the cluster in solvents other than water. ^{11}B NMR was used to determine if the cluster remained intact in the methanol. The ^{11}B NMR of the polycrystals in methanol gave three peaks: 219.597ppm, 218.775ppm, and 216.913ppm indicating that the cluster was present in the solution.

The slow excision of the cluster is due to the bridging of the iodide ligands. The 6-14 stiochiometry which is depicted in Figure 3.2 has a more tightly interlaced network of *inner-ausser* and *ausser-ausser* ligand bridging than do stiochiometries greater than 6-14. In order to excise the cluster these bridging bonds must be broken, which slows the dissolution of individual zirconium clusters from the bulk solid. Water, being extremely polar, is the only solvent with the ability to break the bridging ligand bonds.

Crystal Formation and Characterization: $[Zr_6I_{12}B(CH_3OH)_6][I(CH_3OH)_6]$:

In an attempt to form $[Zr_6I_{12}B]^+$ crystals the polycrystalline material was dissolved in methanol and sealed under vacuum in a Pyrex ampoule and placed in the -20°C freezer overnight. Brown, plate-like crystals formed on the walls of the ampoules. In an inert atmosphere glove box the crystals were removed from the mother liquor and immediately suspended in Apiezon-T grease making them less susceptible to air exposure. A glass fiber made by pulling a heated glass capillary was used to transfer the grease-covered crystals to the goniometer pin. The crystal was placed in a low temperature nitrogen stream at -163°C on a Siemens (Bruker) SMART 2000 CCD X-ray Diffractometer equipped with an LT-2 low temperature apparatus the crystal structure data was collected. A hemisphere of data was collected using an omega scan of 0.3° per frame for 30 seconds. 1257 frames of data were collected with a maximum resolution of 0.75Å. The unit cell parameters of the crystal were obtained using SMART software and further refined using SAINT software. SADABS was used to correct for absorption of x-rays by the plate crystals. The crystal structure was found to be hexagonal with the formula $[Zr_6I_{12}B(CH_3OH)_6][I(CH_3OH)_6]$ and in space group $R\bar{3}$. The cell dimensions were a = 17.7102Å and c = 13.9147Å. There were three cluster molecules per unit cell, Z = 3. The cationic portion of the unit cell, $[Zr_6I_{12}B(CH_3OH)_6]^+$ can be see in Figure 3.4 and the $[I(CH_3OH)_6]^-$ anion can be viewed in Figure 3.5.

The excision and formation of a crystal of the $[Zr_6I_{12}B]^+$ cluster completed the exploration of the family of boron-centered hexazirconium halide clusters. A systematic comparison of structural data indicated some trends in both bond length and bond angle based on the size of the halide ligand in question.

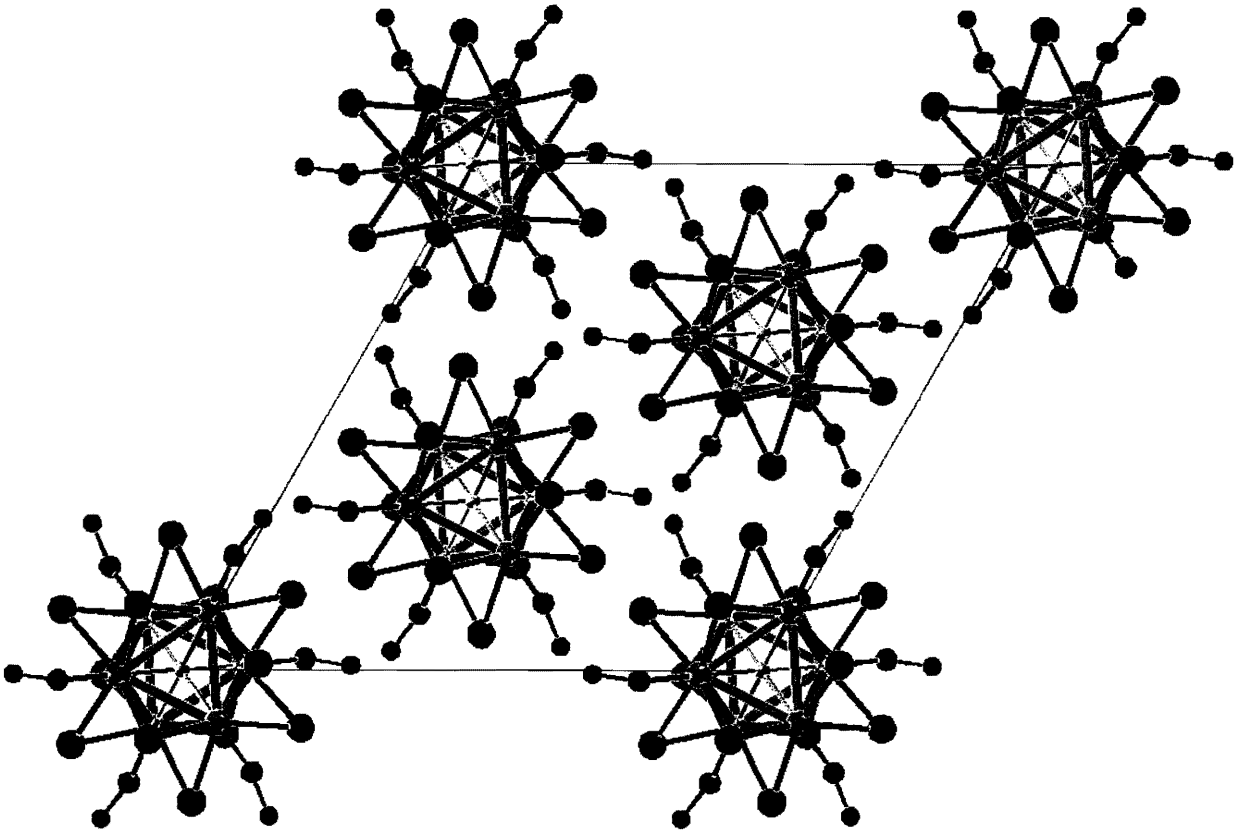

Figure 3.4. The cationic portion of $[Zr_6I_{12}B(CH_3OH)_6][I(CH_3OH)_6]$

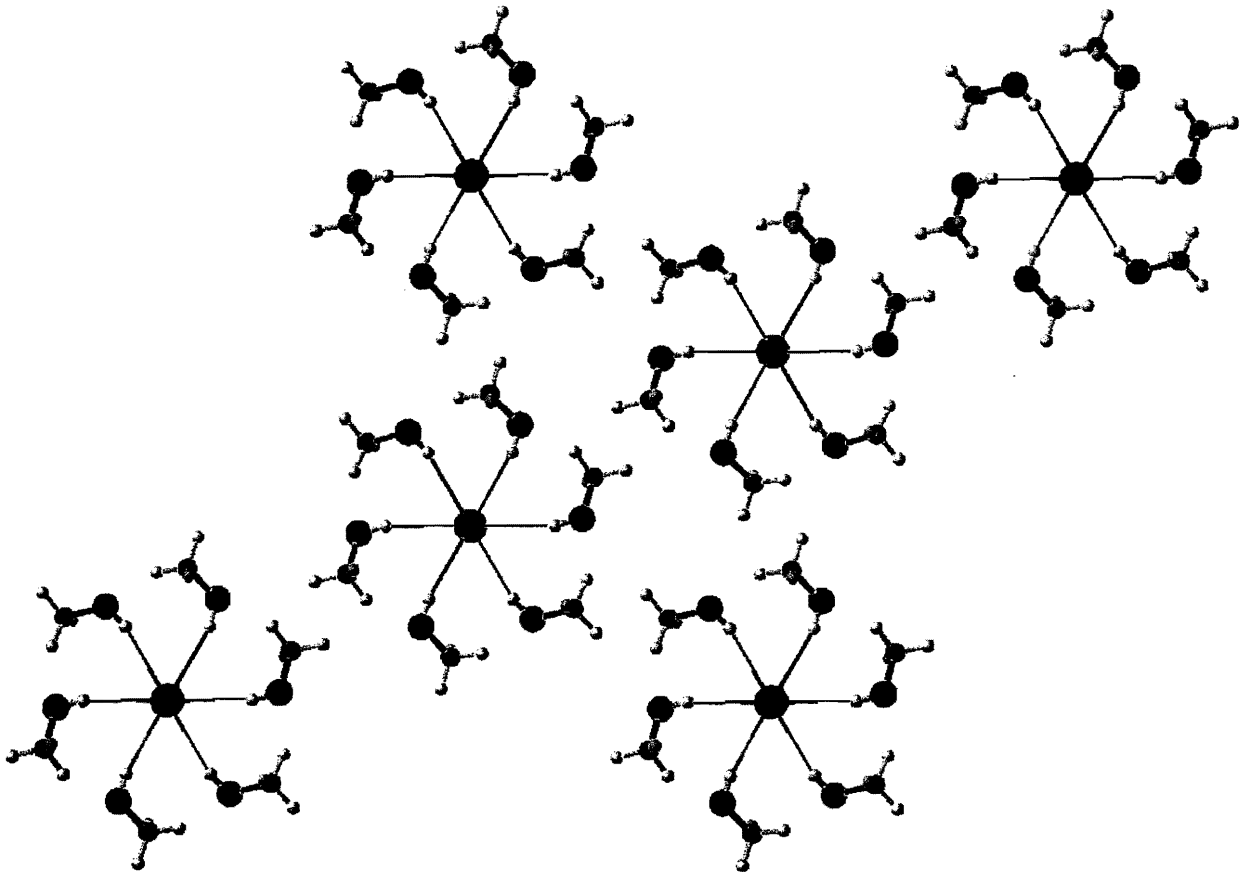

Figure 3.5. The anionic portion of $[Zr_6I_{12}B(CH_3OH)_6][I(CH_3OH)_6]$

Glancing at Table 3.1 one can see that the $[Zr_6I_{12}B]^+$ cluster the average zirconium to halide bond length was determined to be 2.9019(2)Å, while the bond Zr—X bond length was 2.691(1) Å and 2.5512(8)Å for the $[Zr_6Br_{12}B]^+$ and the $[Zr_6Cl_{12}B]^+$ clusters respectively. The zirconium to halide bond length increased with the increased size of the halide, while the X— Zr—X bond angle became more acute. For $[Zr_6Cl_{12}B]^-$ the angle was 169.18(4)° but decreased to 160.81(5) ° for $[Zr_6I_{12}B]^-$. The zirconium to halide bond length was not the only bond length impacted by the size of the halide, but the zirconium to boron bond also increased with halide size. The changes in the cluster's structure are related to its stability. The increased radius of the halide ligands brings greater stability to the cluster by decreasing steric accessibility to the zirconium cage.

Table 3.1. Structural Data for the Family of Boron-centered Hexazirconium Halide Clusters

Cluster	Zr—X bond length (Å)	X—Zr—X bond angle	Zr—B bond length (Å)
$[Zr_6Cl_{12}B]^{+(7)}$	2.5512(8)	169.18(4)°	2.2994(5)
$[Zr_6Br_{12}B]^{+(8)}$	2.691(1)	166.04(4) °	2.3447(8)
$[Zr_6I_{12}B]^{+}$	2.9019(2)	160.81(5) °	2.3779(8)

REFERENCES

1. Fischer, E.O.; Palm, C. *Chem. Ber.* **1958**, *91*, 1725-1731.
2. Barnes, Craig E.; Dial, Michelle R.; and Orvis, Jeffery A. *Organometallics*. **1990**, *9,* 1021-1035.
3. Barnes, Craig E.; Dial, Michelle R. *Organometallics*. **1988**, *7*, 782-784.
4. Barnes, Craig E.; Orvis, Jeffery A. *Journal of the American Chemical Society*. **1989**, *111*, 4992-4994.
5. Sauer, U. H.; Ceska, T. A. *Journal of Applied Crystallography*. **1997**, *30*, 71-72.
6. Xie, Xiaobing; Hughbanks, Timothy. *Angew. Chemistry International Edition English*. **1999**, *38*, 1777-1779.
7. Xie, Xioabing; Reibenspies, Joseph H.; Hughbanks, Timothy. *Journal of the American Chemical Society*. **1998**, *120*, 11391-11400.
8. Xie, Xiaobing; Hughbanks, Timothy. *Inorganic Chemistry*. **2000**, *39,* 555-61.
9. Qi, Ru-Yi; Corbett, John D. *Inorganic Chemistry*. **1995**, *34*, 1646-1651.
10. Cotton, F. A.; Hughbanks, T.; Runyan, C. E. Jr.; Wojtczak, W. A. "Halide Supported Octahedral Clusters of Zirconium:Structural and Bonding Questions." *Early Transition Metal Clusters with Pi-Donor Ligands*. Chisholm, M. H. Ed.; VCH Publishers: New York; **1995**, pp. 1-26.
11. Pinhas, Allan; Albright, Thomas; Hofmann, Peter; Hoffmann, Roald. *Helvetica Chimica Acta*. **1980**, 63, Fasc. 1, Nr. 4, 29-49.

Appendix

APPENDIX

The appendix contains data collected from the x-ray crystallography conducted on $(CoCp)_3(CO)_2$ at seven temperatures in the range of -75° to -157°C. Data collected on the single crystal $[Zr_6I_{12}B(CH_3OH)6][I(CH_3OH)_6]$ will be presented as well.

Crystal Structure Determination of $[Zr_6I_{12}(CH_3OH)_6][I(CH_3OH)_6]$ at –163°C

Structure Determination Summary

Crystal Data

Empirical Formula	$C_{12}\ H_{48}\ B\ I_{13}\ O_{12}\ Zr_6$
Color; Habit	brown plate
Crystal System	Hexagonal
Space Group	$R\bar{3}$
Unit Cell Dimensions	a=17.7102(16)Å
	c=13.9147(17) Å
Volume	3779.6(7) $Å^3$
Z	3
Formula Weight	2412.10 g/mole
Density (calc.)	3.179 Mg/m^3
Absorption Coefficient	8.575 mm^{-1}
F(000)	3211

Data Collection

Diffractometer	Siemens Bruker Smart 2000
Radiation	Mo, k_α=0.71073Å
Temperature	-163°C
Theta Range	3.03 to 23.26°
Limiting Indices	$-19 \le h \le 19, -19 \le k \le 19,$ $-15 \le l \le 10$
Reflections collected	5797
Unique Reflections	1219 (R_{int}=0.1481)
Goodness of Fit on F^2	1.049

Crystal Structure Determination $(CpCo)_3(CO)_2$ at –75°C

Structure Determination Summary

Crystal Data

Empirical Formula	$C_{17}\ H_{15}\ Co_3\ O_2$
Color; Habit	black plate
Crystal System	Hexagonal
Space Group	P6(3)/m
Unit Cell Dimensions	a=9.1500(13)Å
	c=10.714(2) Å
Volume	776.8(2) $Å^3$
Z	2
Formula Weight	428.08 g/mole
Density (calc.)	1.830 Mg/m^3
Absorption Coefficient	3.167 mm^{-1}
F(000)	428

Data Collection

Diffractometer	Siemens Bruker Smart 2000
Radiation	Mo, k_α=0.71073Å
Limiting Indices	$-10 \le h \le 10, -10 \le k \le 9, -11 \le 1 \le 11$
Theta Range	2.57 to 23.20°
Reflections collected	3068
Unique Reflections	398 (R_{int}=0.0567)
Goodness of Fit on F^2	1.121
Residual R1 (all data)	0.0496

Crystal Structure Determination $(CpCo)_3(CO)_2$ at –90°C

Structure Determination Summary

Crystal Data

Empirical Formula	$C_{17}\ H_{15}\ Co_3\ O_2$
Color; Habit	black plate
Crystal System	Hexagonal
Space Group	P6(3)/m
Unit Cell Dimensions	a=9.1560(13)Å
	c=10.650(2) Å
Volume	773.2(2) $Å^3$
Z	2
Formula Weight	428.08 g/mole
Density (calc.)	1.839 Mg/m^3
Absorption Coefficient	3.182 mm^{-1}
F(000)	428

Data Collection

Diffractometer	Siemens Bruker Smart 2000
Radiation	Mo, k_α=0.71073Å
Temperature	-90°C
Theta Range	2.57 to 23.29°
Limiting Indices	$-10 \le h \le 8, -9 \le k \le 10, -11 \le l \le 11$
Reflections collected	2986
Unique Reflections	399 (R_{int}=0.0610)
Goodness of Fit on F^2	1.018
Residual R1 (all data)	0.0581

Crystal Structure Determination $(CpCo)_3(CO)_2$ at –100°C

Structure Determination Summary

Crystal Data

Empirical Formula	$C_{17}\ H_{15}\ Co_3\ O_2$
Color; Habit	black plate
Crystal System	Hexagonal
Space Group	P6(3)/m
Unit Cell Dimensions	a=9.1430(13)Å
	c=10.653(2) Å
Volume	771.2(2) $Å^3$
Z	2
Formula Weight	428.08 g/mole
Density (calc.)	1.843 Mg/m^3
Absorption Coefficient	3.190 mm^{-1}
F(000)	428

Data Collection

Diffractometer	Siemens Bruker Smart 2000
Radiation	Mo, k_α=0.71073Å
Temperature	-100°C
Theta Range	2.57 to 23.23°
Limiting Indices	$-10 \le h \le 10, -10 \le k \le 9, -11 \le l \le 11$
Reflections collected	3020
Unique Reflections	398 (R_{int}=0.0501)
Goodness of Fit on F^2	0.946
Residual R1 (all data)	0.0494

Crystal Structure Determination $(CpCo)_3(CO)_2$ at –110°C

Structure Determination Summary

Crystal Data

Empirical Formula	$C_{17}\ H_{15}\ Co_3\ O_2$
Color; Habit	black plate
Crystal System	Hexagonal
Space Group	P6(3)/m
Unit Cell Dimensions	a=9.1230(13)Å
	c=10.640(2) Å
Volume	766.9(2) $Å^3$
Z	2
Formula Weight	428.08 g/mole
Density (calc.)	1.854 Mg/m^3
Absorption Coefficient	3.208 mm^{-1}
F(000)	428

Data Collection

Diffractometer	Siemens Bruker Smart 2000
Radiation	Mo, k_α=0.71073Å
Temperature	-110°C
Theta Range	2.58 to 23.28°
Limiting Indices	$-10 \le h \le 9, -8 \le k \le 10, -11 \le l \le 11$
Reflections collected	3017
Unique Reflections	398 (R_{int}=0.0506)
Goodness of Fit on F^2	0.988
Residual R1 (all data)	0.0478

Crystal Structure Determination $(CpCo)_3(CO)_2$ at –120°C

Structure Determination Summary

Crystal Data

Empirical Formula	$C_{17}\,H_{15}\,Co_3\,O_2$
Color; Habit	black plate
Crystal System	Hexagonal
Space Group	P6(3)/m
Unit Cell Dimensions	a=9.0930(13)Å
	c=10.573(2) Å
Volume	757.1(2) $Å^3$
Z	2
Formula Weight	428.08 g/mole
Density (calc.)	1.878 Mg/m^3
Absorption Coefficient	3.249 mm^{-1}
F(000)	428

Data Collection

Diffractometer	Siemens Bruker Smart 2000
Radiation	Mo, k_α=0.71073Å
Temperature	-120°C
Theta Range	2.59 to 23.26°
Limiting Indices	$-10 \le h \le 8, -9 \le k \le 10, -11 \le l \le 11$
Reflections collected	2980
Unique Reflections	393 (R_{int}=0.0460)
Goodness of Fit on F^2	1.090
Residual R1 (all data)	0.0505

Crystal Structure Determination $(CpCo)_3(CO)_2$ at –140°C

Structure Determination Summary

Crystal Data

Empirical Formula	$C_{17}\,H_{15}\,Co_3\,O_2$
Color; Habit	black plate
Crystal System	Hexagonal
Space Group	P6(3)/m
Unit Cell Dimensions	a=9.0820(13)Å
	c=10.543(2) Å
Volume	753.1(2) $Å^3$
Z	2
Formula Weight	428.08 g/mole
Density (calc.)	1.888 Mg/m^3
Absorption Coefficient	3.266 mm^{-1}
F(000)	428

Data Collection

Diffractometer	Siemens Bruker Smart 2000
Radiation	Mo, k_α=0.71073Å
Temperature	-140°C
Theta Range	2.59 to 23.24°
Limiting Indices	$-10 \le h \le 9, -10 \le k \le 9, -11 \le l \le 11$
Reflections collected	2948
Unique Reflections	388 (R_{int}=0.0446)
Goodness of Fit on F^2	1.068
Residual R1 (all data)	0.0453

Crystal Structure Determination $(CpCo)_3(CO)_2$ at –157°C

Structure Determination Summary

Crystal Data

Empirical Formula	$C_{17}\,H_{15}\,Co_3\,O_2$
Color; Habit	black plate
Crystal System	Hexagonal
Space Group	P6(3)/m
Unit Cell Dimensions	a=9.0760(13)Å
	c=10.519(2) Å
Volume	750.4(2) $Å^3$
Z	2
Formula Weight	428.08 g/mole
Density (calc.)	1.895 Mg/m^3
Absorption Coefficient	3.278 mm^{-1}
F(000)	428

Data Collection

Diffractometer	Siemens Bruker Smart 2000
Radiation	Mo, k_α=0.71073Å
Temperature	-157°C
Theta Range	2.59 to 23.27°
Limiting Indices	$-10 \le h \le 9, -10 \le k \le 9, -11 \le l \le 11$
Reflections collected	2918
Unique Reflections	388 (R_{int}=0.0430)
Goodness of Fit on F^2	0.892
Residual R1 (all data)	0.0474